Histologic and Biomechanical Evaluation of Alumina-Blasted/Acid-Etched and Resorbable Blasting Media Surfaces

Estevam A. Bonfante, PhD[1]*
Charles Marin, PhD[1]
Rodrigo Granato, PhD[1]
Marcelo Suzuki, DDS[2]
Jenni Hjerppe, DDS[3]
Lukasz Witek, MS[4]
Paulo G. Coelho, PhD[4,5]

This study evaluated the early biomechanical fixation and bone-to-implant contact (BIC) of an alumina-blasted/acid-etched (AB/AE) compared with an experimental resorbable blasting media (RBM) surface in a canine model. Higher texturization was observed for the RBM than for the AB/AE surface, and the presence of calcium and phosphorus was only observed for the RBM surface. Time in vivo and implant surface did not influence torque. For both surfaces, BIC significantly increased from 2 to 4 weeks.

Key Words: biomechanical test, implant surface, resorbable blasting media, roughness

INTRODUCTION

The use of endosseous dental implants is a highly predictable treatment modality supported by a wealth of evidence reporting their safety and high survival rates over the long term.[1] Because the implant surface has been identified as one of the six important factors for implant anchorage in bone,[2] there have been remarkable efforts to improve surface design, as evidenced by the extensive number of studies published since the 1980s. Despite the robust and positive clinical results for turned surfaces, which have been shown to last for up to 20 years,[3] the purpose of changing implant surface topography and/or chemistry is to improve bone healing and reduce the waiting time between implant placement and its functional loading with a prosthesis.[4]

Basically, the engineering processes to modify an implant surface include chemical or physical alterations.[5] Incorporating inorganic phases into the titanium oxide layer, such as calcium phosphate, has been shown to provide higher levels of early biomechanical fixations and bone-to-implant contact (BIC) percentage values compared with as-turned, or grit-blast/acid-etched, surfaces.[6,7] Specific to the addition of calcium- and phosphorus-based materials as coatings, some of the interest is due to the inherent presence of these elemental components in the natural bone. On the other hand, the rationale for making physical modifications is to create a rougher surface at the micrometer level that, up to a certain extent, increases bone anchorage and, at the nanometer scale, increases

[1] UNIGRANRIO, Rio de Janeiro, Brazil.
[2] Department of Prosthodontics, Tufts University School of Dental Medicine, Boston, Mass.
[3] Department of Prosthodontics and Biomaterials Science – Faculty of Medicine, Institute of Dentistry, University of Turku, Turku, Finland.
[4] Department of Biomaterials and Biomimetics, New York University, New York, NY.
[5] Department of Periodontology and Implant Dentistry, New York University College of Dentistry, New York, NY.
* *Corresponding author,* e-mail: estevamab@gmail.com
DOI: 10.1563/AAID-JOI-D-10-00105

surface energy and improves osseointegration.[5–7] However, it is important to bear in mind that surface topography changes with different manufacturing processes; surface chemistry and physics may also be changed, although unintentionally.[8]

Compared with smooth surfaces ($S_a < 0.5$ μm), an increase in surface texture, as observed for moderately rough surfaces (S_a 1.0–2.0 μm), has shown improved bone biological response and mechanical properties.[9–11] Surface texturing can be achieved by a variety of methods, including acid-etching,[12,13] grit-blasting followed by acid-etching, anodization,[14,15] grit-blasting with alumina,[16] titanium oxide,[17] silica,[18,19] or resorbable biocompatible bioceramics (resorbable blasting media [RBM]).[20–22] The goal of the RBM technique is to produce a moderately rough surface by grit-blasting; the bioceramics reduce the likelihood of decreases in biocompatibility due to particle embedding or particle detachment from the surface (RBM is highly biocompatible).[22,23]

Because of past experiences of adhesive failures between the implant device and bioceramic thick coatings, such as plasma-sprayed hydroxiapatite (20–50 μm), and because of its partial dissolution/resorption in vivo,[24–28] smaller-scale bioceramic coatings have been developed. These coatings may involve thickness in the range of a few micrometers or even nanometers, such as the calcium phosphate (CaP) coatings created by discrete crystalline deposition.[29] Early on, the coating dissolution may be influenced in vivo by thickness, micro/nanoscale texturing achievable through any of these processes, and controlled composition. Concerning the residual CaP incorporation by the RBM process, surface topography and chemistry are influenced by blasting media composition; particle size; processing parameters, such as blasting pressure and distance, and subsequent acid-etching treatments.[4] All these parameters may significantly influence the short- and long-term host-to-implant response.

Changes in surface involving the deposition of hydroxiapatite or other CaP compositions result in the surface modification currently investigated most often, altering both chemistry and topography.[8] However, the available evidence supporting the potential value of surface chemical alterations alone, such as CaP, in improving bone response is inconclusive. One claimed contributing factor is the sparse assessment of surface topography and/or chemical alterations performed by appropriate analytical tools,[5] in tandem with in vivo investigations to allow a sound correlation of the interplay between bone response and surface design.[8] Hence, the present study aims to evaluate the effect of an RBM-treated surface, compared with an alumina-blasted/acid-etched (AB/AE) surface in the torque to interface failure and BIC. Surface characterization was performed by three different methods, including scanning electron microscopy (SEM), optical interferometry (IFM), and X-ray photoelectron spectroscopy (XPS). Our tested null hypothesis was that surface treatment would not affect torque or BIC values.

Materials and Methods

The implants used in this study were commercially available Ti-6Al-4V screw-type implants 4 mm in diameter and 13 mm long, which were provided by the manufacturer (ADIN Dental Implants Systems Ltd, Afula, Israel). A total of 56 implants was used and divided into 2 groups according to surface treatment: pure titanium surface treated with RBM as the experimental group ($n = 24$) and an AB/AE group as the control group. The remaining implants were used for surface characterization (4 per group).

Surface characterization

The surface characterization was accomplished with three different methods. First, SEM (Philips XL 30, Eindhoven, The Netherlands) was performed at various magnifications under an acceleration voltage of 15 kV to observe the topography of both surfaces.

The second step was to determine the roughness parameters at the micrometer length scale by optical IFM (Phase View 2.5, Palaiseau, France). For each surface, 3 implants were evaluated, recording S_a (arithmetic average high deviation) and S_q (root mean square) at the flat region of the implant cutting edges (3 measurements per implant) using a filter size of 250 μm × 250 μm. After data normality verification, statistical analysis at the 95% level of significance was performed by 1-way analysis of variance (ANOVA).

The third procedure was the surface-specific chemical assessment performed by XPS. The

implants were inserted in a vacuum transfer chamber and degassed to 10^{-7} torr. The samples were then transferred under vacuum to a Kratos Axis 165 multitechnique XPS spectrometer (Kratos Analytical, Chestnut Ridge, NY). Survey spectra were obtained using a concentric hemispherical analyzer with a 165-mm mean radius operated at a constant pass energy of 160 eV for survey and 80 eV for high-resolution scans. The take-off angle was 90°, and a spot size of 150 μm × 150 μm was used. The implant surfaces were evaluated at various locations.

Animal model and surgical procedure

With the approval of the Ethics Committee for Animal Research at Federal University of Santa Catarina, 12 mongrel dogs were acquired and remained for 2 weeks in the animal facility before the first surgical procedure.

For the surgery, 3 drugs were administered until general anesthesia was achieved by intramuscular injection. The drugs were atropine sulfate (0.044 mg/kg), xilazine chlorate (8 mg/kg), and ketamine chlorate (15 mg/kg). The implantation site was the distal part of the femur (n = 2 per limb); the right limb of each animal provided implants that remained for 4 weeks in vivo, and the left limb provided implants that remained 2 weeks in vivo. For implant placement, the surgical site was shaved with a razor blade, followed by application of antiseptic iodine solution. An incision of ≈5 cm through the skin and periosteum was performed, and the periosteum was elevated for bone exposure. Sequential drills from the manufacturer were used, following the sequence (pilot drill, 2.0 mm, 3.0 mm, and 3.5 mm) under abundant saline irrigation at 1.200 rpm. The implants were placed in an interpolated distribution to minimize bias from different implantation sites and surface type (sites 1 and 2 from proximal to distal) along the distal part of the femur for torque and histomorphometric evaluation. The first implant was placed 1 cm below the joint capsule at the central medial-lateral position of the distal part of the femur. The other devices were placed along the distal direction at distances of 1 cm from each other along the bone. After placement the healing caps were inserted and sutured in layers with vicryl 4-0 (Ethicon Johnson, Miami, Fla) for the periosteum and nylon 4-0 (Ethicon Johnson) for the skin. The animals stayed in the animal care facility and received antibiotics (benzyl penicillin benzatine 20 000 UI/kg) and anti-inflammatory (ketoprofen 1% 1 mL/5 kg) medication to control the pain and infection. Euthanasia was performed after 4 weeks by anesthesia overdose, and the limbs were retrieved by sharp dissection.

According to the initial protocol, half of the specimens of right and left limbs were nondecalcified processed to slides for histomorphologic and histomorphometric (percentage of BIC) evaluation. The other half was subjected to biomechanical testing (torque to interface failure).

At necropsy, the femurs were retrieved by sharp dissection, and surgical blades were used to remove soft tissue. The implants in bone were reduced to blocks and were then immersed in 10% buffered formalin solution for 24 hours. The blocks were then washed in running water for 24 hour and gradually dehydrated in a series of alcohol solutions ranging from 70% to 100% ethanol. After dehydration, the samples were embedded in a methacrylate-based resin (Technovit 9100, Heraeus Kulzer GmbH, Wehrheim, Germany) according to the manufacturer's instructions. The blocks were then cut into slices (~300 μm thick), aiming the center of the implant along its long axis with a precision diamond saw (Isomet 2000, Buehler Ltd, Lake Bluff, Ill), and glued to acrylic plates with an acrylate-based cement. A 24-hour setting time was allowed before grinding and polishing. The sections were then reduced to a final thickness of ~30 μm by means of a series of silicon carbide abrasive papers (400, 600, 800, 1200, and 2400) (Buehler Ltd) in a grinding/polishing machine (Metaserv 3000, Buehler Ltd) under water irrigation.[30] The sections were then stained with toluidine blue and referred to optical microscopy for histomorphologic evaluation.

The BIC was determined at 50×–200× magnification (Leica DM2500M, Leica Microsystems GmbH, Wetzlar, Germany) by means of a computer software program (Leica Application Suite, Leica Microsystems GmbH). The regions of BIC along the implant perimeter were subtracted from the total implant perimeter, and calculations were performed to determine the BIC.

Torque testing required the femur to be adapted to an electronic torque machine equipped with a

200 Ncm load cell (Test Resources, Minneapolis, Minn).

Custom machined tooling was adapted to the internal connection of each implant, and the bone block was carefully positioned to avoid specimen misalignment during testing. The implants were torqued in a counterclockwise direction at a rate of ~0.196 radians/min, and torque versus displacement curve was recorded for each specimen.

Preliminary statistical analyses showed no effect of implant site (ie, there were no consistent effects of implant position along the femur) on all measurements. Therefore, the site was not considered further in the analysis. Further statistical evaluation was performed by ANOVA using implant surface and time in vivo as independent variables and torque and BIC as dependent variables. Statistical significance was indicated by *P* levels less than 5%, and post hoc testing used the Fisher least significant difference test.

Results

The electron micrographs and representative 250 μm × 250 μm IFM three-dimensional reconstructions of the control and experimental implant surfaces are presented in Figures 1 and 2, respectively. Their respective micrometer length scale S_a and S_q values are presented in Figure 3. The surface texture observed at intermediate and high magnification levels did not show evidence of particle embedding in either surface (Figure 1). The micrometer length scale IFM measurements showed higher S_a and S_q values for the experimental surface than for the control surface (Figure 3). The survey XPS spectra detected the presence of

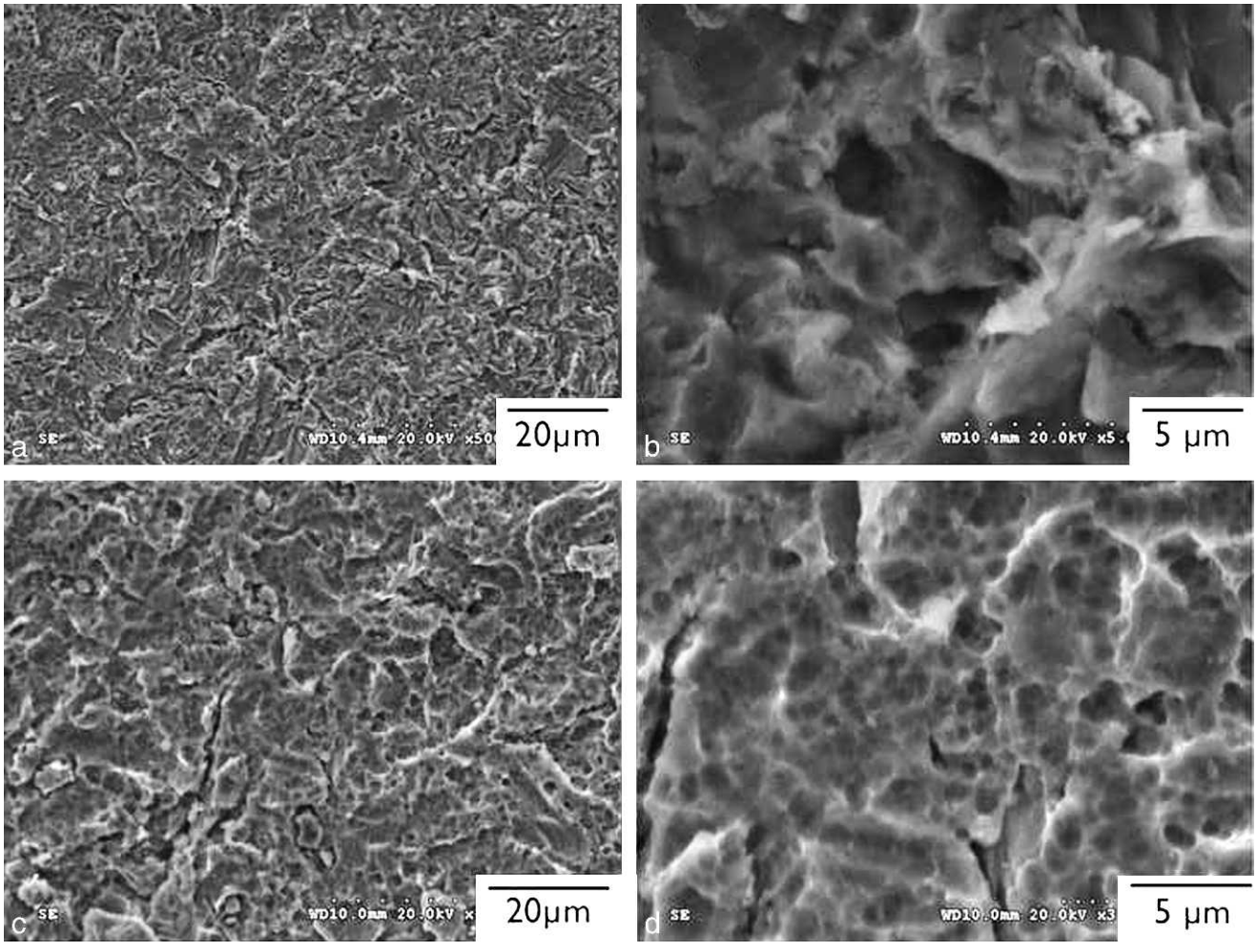

Figure 1. Scanning electron microscopy micrographs show morphology of (a) resorbable blasting media experimental and (c) alumina-blasted/acid-etched control surfaces. Higher magnification of the respective surfaces (b and d) did not reveal evidence of particle embedding in either surface.

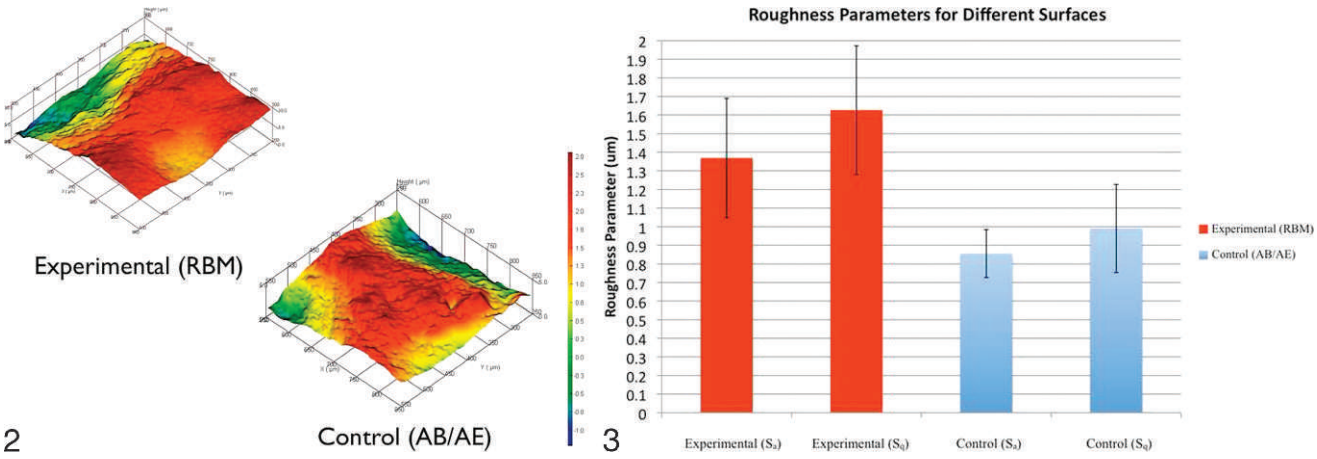

Figures 2 and 3. Figure 2. Micrometer length scale optical interferometry reconstructions showing higher S_a and S_q values for the resorbable blasting media compared with the control surfaces. **Figure 3.** Statistical summary (mean ± 95% CI) of surface roughness parameters at the micrometer level length scale. Statistical *P* values for the experimental S_a and S_q were significantly higher compared with control groups ($P < .05$).

carbon, oxygen, titanium, nitrogen, aluminum, and vanadium for the control surface, and those elements, plus calcium and phosphorus, for the experimental surface (Table 1). Statistical analysis indicated no significant differences between surface types in regards to torque to interface failure and BIC ($P > .71$ and $P > .98$, respectively). Although statistical analysis showed no difference between the times in vivo for torque ($P > .71$), there was statistical difference between BIC and time in vivo ($P < .04$) (Table 2).

Histomorphologic evaluation showed that, irrespective of implant surface, bone to implant response at cortical regions was characterized by woven bone formation and interfacial remodeling at 2 weeks (Figure 4a), followed by its initial replacement by lamellar bone and higher bone organization levels at 4 weeks (Figure 4b). At trabecular regions, a likewise bone to implant response was observed for both surfaces, where woven bone was observed in the vicinity of the implant surfaces at 2 weeks (Figure 5a), and the initial formation of lamellar bone surrounding primary osteonic structures in a higher degree of bone organization was observed at 4 weeks (Figure 5b).

Discussion

The alleged chemical effects of CaP incorporations to an implant surface have long drawn attention as a positive modulator of bone healing. However, whether the subsequent topographical changes contribute alone or in combination with the chemical alterations is still unclear.[8] In the present study, both experimental and control surfaces presented average roughness in the moderately rough range (S_a 1 – 2 μm).[31] Although the roughness of the experimental surface was in the range of what has been shown to result in the strongest bone response (S_a of approximately 1.5 μm)[8,32–34] and was significantly higher than the control surface (S_a of approximately 0.85 μm), torque values were not significantly different at the 2- or 4-week evaluation points. Even though a rougher profile was expected for the control group because the alumina blasting medium was harder than the one used on the experimental group,

Table 1

X-ray photoelectron spectroscopy for the experimental (resorbable blasting media) and control (alumina-blasted/acid-etched) surfaces

Chemical Element	Carbon	Oxygen	Titanium	Neon	Aluminum	Vanadium	Calcium	Phosphorus
Experimental group	38.06	38.65	9.01	0.79	2.28	0.39	0.43	0.67
Control group	40.25	37.79	9.22	1.33	3.97	0.41	-	-

TABLE 2

Statistical summary of torque to interface failure and bone-to-implant contact (BIC) (mean ± 95% CI) for the different surfaces (Torque $P > .71$, BIC $P > .98$) and times in vivo (Torque $P > .54$, BIC $P < .04$).

Independent Variable	Torque (Ncm)	95% CI	BIC (%)	95% CI
Experimental Surface	121.78	±20.13	33.67	±6.24
Control Surface	126.73	±20.14	33.74	±6.25
2 weeks	120.01	±21.08	28.98	±6.24
4 weeks	128.51	±19.24	38.43	±6.25

several other parameters, such as pressure, distance, particle size, and subsequent acid etching, may result in a wide range of surface roughness measurements for control implants. As no information regarding the manufacturing process of both surfaces was provided by the manufacturer, further comments on how such surface characteristics were achieved would be speculative in nature. However,

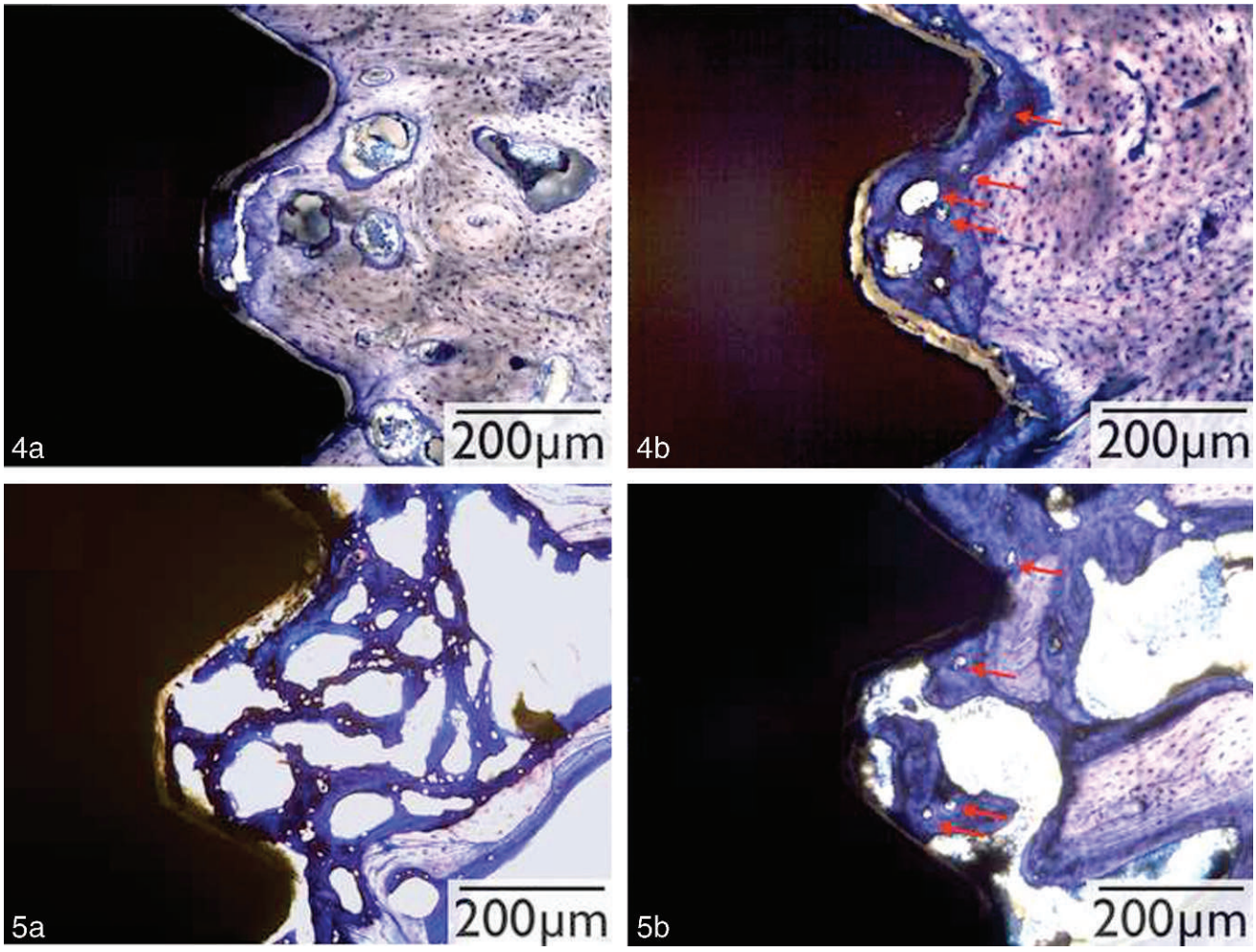

FIGURES 4 AND 5. FIGURE 4. Optical microscopy revealed similar bone to implant response for both experimental (PTS) and control (RED) surfaces at cortical regions, where (a) woven bone along with interfacial remodeling was observed in proximity with the implant surfaces at 2 weeks, and (b) higher degrees of bone organization were observed at 4 weeks, where partial replacement of woven bone by lamellar bone was observed (arrows). Toluidine blue stained. **FIGURE 5.** Optical microscopy revealed similar bone to implant response for both experimental (PTS) and control (RED) surfaces at trabecular regions, where (a) woven bone was observed in proximity with the implant surfaces at 2 weeks, and (b) higher degrees of bone organization were observed at 4 weeks, where lamellar bone surrounding primary osteonic structures was observed (arrows). Toluidine blue stained.

from a surface chemistry standpoint, both surfaces presented elemental composition similar to the composition presented in previous studies.[21,22,35]

Time in vivo significantly increased BIC values proportionally for both surfaces. The temporal increase for BIC values only and not for torque suggests that static histomorphometric parameters, such as BIC, present weak evidence of a better implant bone interface or biomechanical fixation. It has been previously emphasized that less BIC in a higher-magnitude mechanical property supporting bone may be preferred over a device with more BIC presenting bone with lower magnitude mechanical properties.[4] Hence, BIC is a measurable parameter with important but limited significance when considering its implication in biomechanical testing such as torque.

Our imaging results showed similar surface-texture morphology for both surfaces at intermediate and high magnification levels in the SEM and IFM reconstructions. Although the micrometer length scale IFM measurements showed higher S_a and S_q values for the experimental surface than for the control, and no differences in torque and BIC were observed, an investigation where only nanometer roughness was compared with a micrometer scale control showed stronger bone response for the former surface, and in that study chemistry was ruled out as the explanatory factor.[36] When a nano-capped surface (approximately 20 nm) was compared to a polished titanium surface in a different experiment by the same group, stronger bone response was observed for the nano-surface.[37] However, whether surface chemistry modification, the presence of nano-roughness, or the combination of both factors fostered bone to implant response (and to what extent) is unknown.

The histomorphologic sections depicted bone in close contact with the implant surface in both trabecular and cortical bone for both experimental and control surfaces, indicating their biocompatible and osseoconductive potential. The healing pathway observed in the present study was similar to what has been described for screw-root form implants, where woven bone was observed around both surfaces at 2 weeks, followed by its initial replacement by lamellar bone at 4 weeks.[9,22,38]

Based on the results, surface treatment did not affect torque or BIC values at early implantation times, leading to the acceptance of our postulated null hypothesis. Both surfaces presented equivalent histomorphologic, histomorphometric, and mechanical testing outcomes despite significant differences in surface roughness and varied chemical composition. The fact that both surfaces presented different roughness and chemistry profiles is a limitation of the present study; thus, controlled experimental designs where both roughness and chemistry are varied in a controlled fashion, along with an appropriate systematic surface classification as proposed by Dohan Ehrenfest et al, would be desirable.[5] The interplay between roughness and/or chemical alterations and their individual contribution to osseointegration is not yet understood.

Abbreviations

AB/AE: alumina-blasted/acid-etched
ANOVA: analysis of variance
BIC: bone-to-implant contact
CaP: calcium phosphate
IFM: interferometry
RBM: resorbable blasting media
SEM: scanning electron microscopy
XPS: X-ray photoelectron spectroscopy

References

1. Berglundh T, Persson L, Klinge B. A systematic review of the incidence of biological and technical complications in implant dentistry reported in prospective longitudinal studies of at least 5 years. *J Clin Periodontol*. 2002;29(suppl 3):197–212; discussion 32–33.

2. Albrektsson T, Branemark PI, Hansson HA, Lindstrom J. Osseointegrated titanium implants. Requirements for ensuring a long-lasting, direct bone-to-implant anchorage in man. *Acta Orthop Scand*. 1981;52:155–170.

3. Lekholm U, Grondahl K, Jemt T. Outcome of oral implant treatment in partially edentulous jaws followed 20 years in clinical function. *Clin Implant Dent Relat Res*. 2006;8:178–186.

4. Coelho PG, Granjeiro JM, Romanos GE, et al. Basic research methods and current trends of dental implant surfaces. *J Biomed Mater Res B Appl Biomater*. 2009;88:579–596.

5. Dohan Ehrenfest DM, Coelho PG, Kang BS, Sul YT, Albrektsson T. Classification of osseointegrated implant surfaces: materials, chemistry and topography. *Trends Biotechnol*. 2010;28:198–206.

6. Albrektsson T, Wennerberg A. Oral implant surfaces: part 1—review focusing on topographic and chemical properties of different surfaces and in vivo responses to them. *Int J Prosthodont*. 2004;17:536–543.

7. Lemons J, Dietch-Misch F. Biomaterials for dental implants. In: Misch CE, ed. *Contemporary Implant Dentistry*. St Louis, Mo: Mosby; 1999;271–302.

8. Wennerberg A, Albrektsson T. Structural influence from calcium phosphate coatings and its possible effect on enhanced bone integration. *Acta Odontol Scand*. 2009;67:333–340.

9. Abrahamsson I, Berglundh T, Linder E, Lang NP, Lindhe J. Early bone formation adjacent to rough and turned endosseous implant surfaces. An experimental study in the dog. *Clin Oral Implants Res*. 2004;15:381–392.

10. Grizon F, Aguado E, Hure G, Basle MF, Chappard D. Enhanced bone integration of implants with increased surface roughness: a long term study in the sheep. *J Dent*. 2002;30:195–203.

11. Wennerberg A, Albrektsson T. On implant surfaces: a review of current knowledge and opinions. *Int J Oral Maxillofac Implants*. 2010;25:63–74.

12. Butz F, Aita H, Wang CJ, Ogawa T. Harder and stiffer bone osseointegrated to roughened titanium. *J Dent Res*. 2006;85:560–565.

13. Klokkevold PR, Nishimura RD, Adachi M, Caputo A. Osseointegration enhanced by chemical etching of the titanium surface. A torque removal study in the rabbit. *Clin Oral Implants Res*. 1997;8:442–447.

14. Huang YH, Xiropaidis AV, Sorensen RG, Albandar JM, Hall J, Wikesjo UM. Bone formation at titanium porous oxide (TiUnite) oral implants in type IV bone. *Clin Oral Implants Res*. 2005;16:105–111.

15. Jungner M, Lundqvist P, Lundgren S. Oxidized titanium implants (Nobel Biocare TiUnite) compared with turned titanium implants (Nobel Biocare mark III) with respect to implant failure in a group of consecutive patients treated with early functional loading and two-stage protocol. *Clin Oral Implants Res*. 2005;16:308–312.

16. Suzuki M, Guimaraes MV, Marin C, Granato R, Gil JN, Coelho PG. Histomorphometric evaluation of alumina-blasted/acid-etched and thin ion beam deposited bioceramic surfaces: an experimental study in dogs. *J Oral Maxillofac Surg*. 2009;67:602–607.

17. Vercaigne S, Wolke JG, Naert I, Jansen JA. A mechanical evaluation of TiO2-gritblasted and Ca-P magnetron sputter coated implants placed into the trabecular bone of the goat: part 1. *Clin Oral Implants Res*. 2000;11:305–313.

18. Albrektsson T, Wennerberg A. Oral implant surfaces: part 2—review focusing on clinical knowledge of different surfaces. *Int J Prosthodont*. 2004;17:544–564.

19. Buser D, Broggini N, Wieland M, et al. Enhanced bone apposition to a chemically modified SLA titanium surface. *J Dent Res*. 2004;83:529–533.

20. Coelho PG, Lemons JE. Physico/chemical characterization and in vivo evaluation of nanothickness bioceramic depositions on alumina-blasted/acid-etched Ti-6Al-4V implant surfaces. *J Biomed Mater Res A*. 2009;90:351–361.

21. Marin C, Granato R, Suzuki M, Gil JN, Piattelli A, Coelho PG. Removal torque and histomorphometric evaluation of bioceramic grit-blasted/acid-etched and dual acid-etched implant surfaces: an experimental study in dogs. *J Periodontol*. 2008;79:1942–1949.

22. Marin C, Granato R, Suzuki M, et al. Biomechanical and histomorphometric analysis of etched and non-etched resorbable blasting media processed implant surfaces: an experimental study in dogs. *J Mech Behav Biomed Mater*. 2010;3:382–391.

23. Lacefield WR. Current status of ceramic coatings for dental implants. *Implant Dent*. 1998;7:315–322.

24. deGroot KKC, Wolke JGC, deBieck-Hogervorst JM. Plasma-sprayed coating of calcium phosphate. In: Yamamuro THL, Wilson J, eds. *Handbook of Bioactive Ceramics, vol II. Calcium Phosphate and Hydroxyapatite Ceramics*. Boca Raton, Fla: CRC Press; 1990;17–25.

25. Kay J. Calcium phosphate coatings for dental implants. *Dent Clin North Am*. 1992;36:1–18.

26. Lacefield WR. Hydroxyapatite coatings. *Ann N Y Acad Sci*. 1988;523:72–80.

27. Ong JL, Carnes DL, Bessho K. Evaluation of titanium plasma-sprayed and plasma-sprayed hydroxyapatite implants in vivo. *Biomaterials*. 2004;25:4601–4606.

28. Yang Y, Kim KH, Ong JL. A review on calcium phosphate coatings produced using a sputtering process—an alternative to plasma spraying. *Biomaterials*. 2005;26:327–337.

29. Orsini G, Piattelli M, Scarano A, et al. Randomized, controlled histologic and histomorphometric evaluation of implants with nanometer-scale calcium phosphate added to the dual acid-etched surface in the human posterior maxilla. *J Periodontol*. 2007;78:209–218.

30. Donath K, Breuner G. A method for the study of undecalcified bones and teeth with attached soft tissues. The Sage-Schliff (sawing and grinding) technique. *J Oral Pathol*. 1982;11:318–326.

31. Wennerberg A, Albrektsson T. Effects of titanium surface topography on bone integration: a systematic review. *Clin Oral Implants Res*. 2009;20(suppl 4):172–184.

32. Wennerberg A, Albrektsson T, Andersson B. An animal study of cp titanium screws with different surface topographies. *J Mater Sci Mater Med*. 1995;6:302–309.

33. Wennerberg A, Albrektsson T, Andersson B, Krol JJ. A histomorphometric and removal torque study of screw-shaped titanium implants with three different surface topographies. *Clin Oral Implants Res*. 1995;6:24–30.

34. Wennerberg A, Albrektsson T, Johansson C, Andersson B. Experimental study of turned and grit-blasted screw-shaped implants with special emphasis on effects of blasting material and surface topography. *Biomaterials*. 1996;17:15–22.

35. Kang BS, Sul YT, Oh SJ, Lee HJ, Albrektsson TXPS. AES and SEM analysis of recent dental implants. *Acta Biomater*. 2009;5:2222–2229.

36. Meirelles L, Melin L, Peltola T, et al. Effect of hydroxyapatite and titania nanostructures on early in vivo bone response. *Clin Implant Dent Relat Res*. 2008;10:245–254.

37. Meirelles L, Arvidsson A, Andersson M, Kjellin P, Albrektsson T, Wennerberg A. Nano hydroxyapatite structures influence early bone formation. *J Biomed Mater Res A*. 2008;87:299–307.

38. Berglundh T, Abrahamsson I, Lang NP, Lindhe J. De novo alveolar bone formation adjacent to endosseous implants. *Clin Oral Implants Res*. 2003;14:251–262.